


## ORIGINAL ARTICLE

# Frequently expressed glypican-3 as a promising novel therapeutic target for osteosarcomas

Jun-Hua Nie<sup>1</sup> | Tao Yang<sup>2</sup> | Hong Li<sup>3</sup> | Sheng Li<sup>3</sup> | Ting-Ting Li<sup>3</sup> | Hai-Shan Ye<sup>1</sup> | Meng-Di Lu<sup>1</sup> | Xiao Chu<sup>2</sup> | Guo-Qing Zhong<sup>2</sup> | Jie-Long Zhou<sup>2</sup> | Mo-Li Wu<sup>4</sup> | Yu Zhang<sup>2</sup> | Jia Liu<sup>1,4</sup> 

<sup>1</sup>South China University of Technology School of Medicine, Guangzhou, China

<sup>2</sup>Department of Orthopedic Oncology, Guangdong Provincial People's Hospital Affiliated to South China University of Technology School of Medicine, Guangzhou, China

<sup>3</sup>BioMed Laboratory, Guangzhou Jingke Biotech Group, Guangzhou, China

<sup>4</sup>Liaoning Laboratory of Cancer Genomics and Epigenomics, College of Basic Medical Sciences, Dalian Medical University, Dalian, China

## Correspondence

Jia Liu, Department of Cell Biology, School of Medicine, South China University of Technology (SCUT), Guangzhou 510000, China.

Email: [mcliujia@scut.edu.cn](mailto:mcliujia@scut.edu.cn)

Yu Zhang, Department of Orthopedic Oncology, Guangdong Provincial People's Hospital, School of Medicine, South China University of Technology, Guangzhou 510030, China.

Email: [zhangyu@gdph.org.cn](mailto:zhangyu@gdph.org.cn)

## Funding information

Central Government of China; the High-level Hospital Construction Project of China, Grant/Award Number: DFJH201905; National Natural Science Foundation of China, Grant/Award Number: 81450016, 81272786 and 31771038

## Abstract

Osteosarcoma (OS) is the most common bone malignancy without a reliable therapeutic target. Glypican-3 (GPC3) mutation and upregulation have been detected in multidrug resistant OS, and anti-GPC3 immunotherapy can effectively suppress the growth of organoids. Further profiling of GPC3 mutations and expression patterns in OS is of clinical significance. To address these issues, fresh OS specimens were collected from 24 patients for cancer-targeted next-generation sequencing (NGS) and three-dimensional patient-derived organoid (PDO) culture. A tumor microarray was prepared using 37 archived OS specimens. Immunohistochemical (IHC) staining was performed on OS specimens and microarrays to profile GPC3 and CD133 expression as well as intratumoral distribution patterns. RT-PCR was conducted to semiquantify GPC3 and CD133 expression levels in the OS tissues. Anti-GPC3 immunotherapy was performed on OS organoids with or without GPC3 expression and its efficacy was analyzed using multiple experimental approaches. No OS cases with GPC3 mutations were found, except for the positive control (OS-08). IHC staining revealed GPC3 expression in 73.77% (45/61) of OSs in weak (+; 29/45), moderate (++; 8/45), and strong (+++; 8/45) immunolabeling densities. The intratumoral distribution of GPC3-positive cells was variable in the focal (+; 10%–30%; 8/45), partial (++; 31%–70%; 22/45), and the most positive patterns (+++; >71%; 15/45), which coincided with CD133 immunolabeling ( $P = 9.89 \times 10^{-10}$ ). The anti-GPC3 antibody efficiently inhibits Wnt/ $\beta$ -catenin signaling and induces apoptosis in GPC3-positive PDOs and PDXs, as opposed to GPC3-negative PDOs and PDXs. The high frequency of GPC3 and CD133 co-expression and the effectiveness of anti-wild-type GPC3-Ab therapy in GPC3-positive OS models suggest that GPC3 is a novel prognostic parameter and a promising therapeutic target for osteosarcoma.

**Abbreviations:** CAR T, chimeric antigen receptor T cell; GPC3, glypican-3; GPC3-Ab, anti-GPC3-antibody; GPC3-AS1, lncRNA glypican 3 antisense transcript 1; HCC, hepatocellular carcinoma; IF, immunofluorescence; IHC, immunohistochemistry; NAC, neoadjuvant chemotherapy; NGS, next-generation sequencing; OS, osteosarcoma; OSDX, OS-derived xenograft; OSO, osteosarcoma organoid; PDO, patient-derived organoids; PDX, patient-derived xenograft; SGBS, Simpson-Golabi-Behmel syndrome; SNP, single nucleotide polymorphism.

This is an open access article under the terms of the [Creative Commons Attribution-NonCommercial-NoDerivs](https://creativecommons.org/licenses/by-nc-nd/4.0/) License, which permits use and distribution in any medium, provided the original work is properly cited, the use is non-commercial and no modifications or adaptations are made.

© 2022 The Authors. *Cancer Science* published by John Wiley & Sons Australia, Ltd on behalf of Japanese Cancer Association.

## KEYWORDS

CD133, gene expression, GPC3, immunotherapy, osteosarcoma, patient-derived organoids, patient-derived xenograft, targeted therapy, Wnt/ $\beta$ -catenin pathway

## 1 | INTRODUCTION

Osteosarcoma (OS) is the most common primary bone malignancy, and often occurs in childhood.<sup>1</sup> In general, the prognosis of OS is poor because of the difficulty in radically removing the tumor, the heterogeneous response of OS cells to chemotherapy, and frequent tumor dissemination.<sup>2</sup> Consequently, the 5-year survival rate of patients with OS is the second lowest among childhood malignancies.<sup>3</sup> Moreover, 80% of patients with OS have undetectable micrometastases at the time of diagnosis, resulting in a high risk of tumor relapse and poor prognosis.<sup>4</sup> For these reasons, NAC is often used before surgery to localize the tumor mass and eliminate potential metastatic focus.<sup>5</sup> Although aggressive NAC has increased the overall survival rate of localized OS, the poor survival rates for patients with OS with metastasis or recurrence have remained almost unchanged in recent years.<sup>6</sup> In this context, there is an urgent need to explore new molecular targets to improve the therapeutic outcomes of patients with OS, especially those with metastases and tumor relapse.

Next-generation genomic sequencing (NGS) has been widely used for personalized therapy to detect drug targets according to genomic alterations in individual patients.<sup>7-9</sup> However, only 0.4% of the detected gene mutations can be used as FDA-approved targeted drugs, and 9.6% as potential therapeutic targets.<sup>10</sup> For osteosarcomas, no targetable mutations have been detected to date and, as a consequence, no OS-targeted therapy is currently available.<sup>11</sup> Recently, our genome-wide NGS sequencing revealed a *GPC3* mutation in an OS case ("OS-8" in our case list) as well as its increased mutation abundance and expression level in the corresponding metastatic tumor.<sup>12</sup> *GPC3* encodes a carcinoembryonic protein and is actively involved in the carcinogenesis of human HCCs.<sup>13</sup> Due to the importance of *GPC3* in HCC cell growth and survival, anti-*GPC3* immunotherapy has been applied in clinical trials for HCCs.<sup>14,15</sup> Therefore, this strategy has been used to treat organoids derived from metastatic OS-8 specimens with *GPC3* mutations and has achieved promising inhibitory effects.<sup>12</sup> These findings indicate that *GPC3* may be a potential therapeutic target for OS if it is frequently mutated and/or expressed in this type of bone malignancy.

This study aimed to address whether *GPC3* mutation and upregulation is an occasional event that occurs in an individual case or a general feature of OS using 61 OS specimens. A panel of OS-derived organoids (OSO) and a high *GPC3* expressing OS-derived xenograft (OSDX) model were established, by which the immunotherapeutic value of *GPC3* in OS management was elucidated by evaluating the response of *GPC3*-positive and *GPC3*-negative OS cells to anti-*GPC3* treatment. Therefore, the biological importance and therapeutic value of *GPC3* in OSs can be clarified.

## 2 | MATERIALS AND METHODS

### 2.1 | Sample collection and tissue microarray construction

Fresh OS specimens were obtained within 20 min of surgical removal. In total, 24 OS samples were collected from primary growth sites using bone puncture biopsy at the time of diagnosis or during surgery after neoadjuvant chemotherapy. Part of each specimen was used for pathological diagnosis, and the remainder for three-dimensional organoid culture, immunohistochemical staining, and nucleic acid isolation, according to existing methods.<sup>16,17</sup> In addition, 37 archived OS cases with definite pathological diagnosis and clinical staging were selected for OS tissue microarray construction according to preexisting methods.<sup>18</sup> Briefly, OS tissue paraffin blocks were sliced into 7- $\mu$ m sections and subjected to H&E morphological staining to determine the representative tumor regions for tissue microarray construction (Chinese Inventive Patent: 02109826.3). The tissue microarray harboring 74 cored tissue pillars from 37 OS cases was prepared and serially sectioned in 7- $\mu$ m slices on a microtome (Leica, RM2245) for high throughput immunohistochemical analysis.

### 2.2 | Immunohistochemical profiling of *GPC3* expression in osteosarcomas

Paraffin sections from 24 patients and OS tumor microarrays were used for IHC. Next, 37 OS cases with clear pathological diagnoses and detailed clinical staging were selected for OS tissue microarray construction using existing methods.<sup>18</sup> IHC was performed using two anti-*GPC3* antibodies (Abcam, ab207080, UK, rabbit monoclonal-Ab, 1:500; Bioss, B0055R, USA, mouse monoclonal-Ab, 1:500) according to previously described methods.<sup>19</sup> According to the labeling intensities, the results were graded as negative (-) if no immunolabeling was observed in the tumor cells, weakly positive (+) if the labeling was faint, moderately positive (++) or strongly positive (+++) when the labeling was stronger or distinctly stronger than (++)<sup>20</sup> According to the percentage of *GPC3*-positive tumor cells in the OS tissues, the staining results were grouped as negative (-, <10%), focal positive (+, 11%–30%), partially positive (++, 31%–70%), and the most positive (+++, >71%).<sup>13,21</sup>

### 2.3 | Tumor NGS sequencing

Tumor NGS was performed as described in the published literature.<sup>12</sup> The sequencing coverage and quality statistics for each sample are summarized in Table S1 and uploaded to the Sequence Read

Archive under the accession number NCBI: PRJNA774097. The 548 genes identified in this array are listed in Table S2.

## 2.4 | RT-PCR and GPC3 transcriptome sequencing

RT-PCR was performed according to existing methodology.<sup>12</sup>

## 2.5 | Organoid modeling

Fresh OS samples from 24 patients were washed with phosphate-buffered saline (PBS) (Gibco, 14190250) containing 500 U penicillin, 500 µg/ml streptomycin, and 50 µg/ml nystatin three times, and then cut into small pieces (<0.1 mm diameter) in a suitable amount of ice-cold medium. The minced tissues were digested in 1 ml TrypLE (Gibco, A1217701) for 45 min at 37°C, washed three times with culture medium, and filtered through a 70-µm cell strainer to remove large undigested fragments. The filtered solution was centrifuged at 300 rpm for 5 min before the cell pellet was resuspended in complete culture medium and mixed with a 1:2 volume of phenol red-free Matrigel matrix (Corning, 356237). Next, 10,000–20,000 cells/30 µl of droplets were plated in a 48 well plate. After allowing the Matrigel to polymerize, 300 µl complete culture medium was added to each well and the samples incubated under conventional cell culture conditions. The culture medium was changed every 2 days. The complete culture medium for OS organoids contained DMEM/F12 with L-glutamine and sodium bicarbonate (Gibco, 12634010), 10% fetal bovine serum (FBS; Australia, Gibco, 10099141), 100 U/ml penicillin, 100 µg/ml streptomycin (Gibco, 15070063), 20 µg/ml nystatin (Sangon Biotech, 89104730), 10 mM nicotinamide (Sigma, N0636), 1 mM N-acetylcysteine (Sigma, 106425), 0.5 µM A83-01 (Tocris, 909910), 1× B-27 minus vitamin A (Invitrogen, 12587010), 50 ng/ml epidermal growth factor (EGF) (Peprotech, AF-100-15), 500 ng/ml RSP01 (Peprotech, 120-38), 10 µM SB-202190 (Sigma, 152121), 10 µmol/L ROCK inhibitor Y-27632 (Sigma Aldrich, HY-10071), and 100 ng/ml Noggin (Medical Chemical Express, HY-P7086).

## 2.6 | CD133 and GPC3 double immunofluorescent labeling

Double immunofluorescent labeling (IF) was performed according to methods described previously.<sup>12</sup>

## 2.7 | Anti-GPC3 therapy of OS organoids

Drug sensitivity assays were performed on OS organoids from five GPC3-positive cases and one GPC3-negative case using 2 µg/ml anti-glypican-3/GPC3 mouse monoclonal antibody (Cell

Marque, 261M-94) for 96 h. OSOs treated with the antibody diluent (938B-03; Cell Marque) were used as the background control. Following calcein/propidium iodide (PI) cell viability, 5-ethynyl-2'-deoxyuridine (EdU) cell proliferation, and terminal deoxynucleotidyl transferase dUTP nick end labeling (TUNEL) apoptotic cell labeling were performed, as described previously.<sup>12</sup> More than 30 OSOs of ~100 µm in diameter were selected from each experimental group for calcein/PI-based viable/nonviable cell counting, which was repeated three times to establish a confidential conclusion.

## 2.8 | Establishment of a GPC3 expressing OSDX model

The animal experimental protocol was examined and approved by the Animal Ethics Committee of Guangdong Provincial People's Hospital (No. GDREC2020093A) before the experiments were conducted. Here, 4- to 6-week-old male NOD/SCID mice with homozygous SCID mutations were obtained from GemPharmatech Co. Ltd. All animal experiments conformed to regulatory standards and the animals were well cared for. Fresh osteosarcoma tissue was collected from a male 8-year-old patient after obtaining informed consent from the patient's parents. This OS case (OS-1) was diagnosed as a moderately differentiated osteoblastic osteosarcoma. The tissue was aseptically cut into approximately 2×2 mm pieces and placed in ice-cold DMEM/F12 medium for transplantation using previously described methods.<sup>22</sup> Briefly, one or two small tissue pieces were implanted subcutaneously at one or two sites on the backs of NOD/SCID mice using a trocar. When the size of the transplanted tumors reached 1.0–1.5 cm, tumors were removed from the local growth sites and serial transplantation was conducted in the same manner as described above. The OSDX model, OSDX-1, was frozen in a biobank and underwent three passages at the time of the experiment.

## 2.9 | Treatment of OSDX-bearing mice with anti-GPC3 antibody

After passaging three times, five pieces of xenograft tissue were inoculated subcutaneously into the mice for *in vivo* anti-GPC3-Ab treatment. When the average tumor volume ( $V = ab^2/2$ ;  $a$  = largest axis,  $b$  = smallest axis<sup>23</sup>) reached >150 mm<sup>3</sup>, the tumor-bearing mice were divided randomly into two experimental groups ( $n = 5$ ): the antibody diluent control group and the anti-GPC3-Ab-treated group. As shown in Figure 6, GPC3-Ab (Cell Marque, 261M-94) was intravenously administered at a dose of 100 µg/mouse on days 0, 7, and 14.<sup>24</sup> An equal volume of antibody diluent was used as the control. Tumor sizes were monitored at 3–4 day intervals using a digital caliper. At 28 days after treatment, the mice were sacrificed by an animal expert, and the tumors were harvested from both groups,

photographed, weighed, and analyzed using different experimental approaches.

## 2.10 | Western blot analysis of GPC3-Ab-treated OSDXs

GPC3-Ab can disrupt the canonical Wnt/ $\beta$ -catenin signaling cascade by inhibiting the interaction between GPC3 and WNT3a and reducing access of the ligand to the frizzled receptors.<sup>25</sup> To assess the influence of GPC3-Ab on the canonical Wnt/ $\beta$ -catenin pathway, total cellular proteins of GPC3-Ab and GPC3-Ab diluent-treated OSDXs were prepared respectively 28 days after treatment. Briefly, using frozen tissue sections, 20 target fragments were placed in a tube containing 50  $\mu$ l strong RIPA lysis buffer (Beyotime). After homogenization using ultrasonic vibration, the samples were heated in boiling water for 5 min. For western blot analysis, the tumor tissue proteins (20  $\mu$ g/well) were separated using electrophoresis in 10% sodium dodecylsulfate-polyacrylamide gel, before being transferred onto a polyvinylidene difluoride membrane (Amersham, Buckinghamshire, UK). The membrane was blocked with 5% skimmed milk (Sigma Aldrich, 1.15363) in PBS and incubated overnight at 4°C with rabbit anti-human active  $\beta$ -catenin monoclonal antibody (1:1000; Cell Signaling Technology, 19807S), total  $\beta$ -catenin rabbit monoclonal antibody (1:1000; Cell Signaling Technology, 8480S), or a rabbit anti-human GAPDH polyclonal antibody (1:10000; Proteintech, 10494-1-AP), followed by incubation with HRP-conjugated goat anti-rabbit IgG (Absin Bioscience, abs20002). Bound antibodies were detected using an Amersham Imager 600 series (GE Healthcare). Quantitative analysis was performed using ImageJ software (Java, National Institutes of Health).

## 2.11 | Statistical analyses

The experimental data are expressed as mean  $\pm$  standard deviation. SPSS software V26.0 was used for further statistical analyses. Statistical significance was set at  $p < 0.05$ .

# 3 | RESULTS

## 3.1 | Rarity of GPC3 mutation in OS specimens

Genomic DNA samples were prepared using fresh OS specimens from 24 patients and subjected to cancer-targeted NGS, which covered 548 cancer-related genes.<sup>26</sup> The results reveal that each DNA sample harbored the wild-type rather than the mutant *GPC3* gene, except OS08, which had a *GPC3* mutation and was cited as the positive control (Figure 1A). The 271bp *GPC3* RT-PCR products were generated in the majority of OSs checked (Figure 1B), and Sanger sequencing showed that the *GPC3* mRNA harboring the G to A mutation at 1046 in exon 4 was transcribed only in OS-08 and wild-type *GPC3* was expressed in the other OS (Figure 1C).

## 3.2 | Frequent GPC3 expression in osteosarcomas rather than osteocytes

The *GPC3* expression patterns of 61 osteosarcoma cases were profiled using immunohistochemical (IHC) staining and scored according to the presence and generality of *GPC3* immunological labeling (Table 1). The reliability of *GPC3* staining was ascertained using anti-*GPC3*-Abs from Abcam (ab207080) and BioMosaics (B0025R; Figure 2A). As shown in Figure 2B and summarized in Table 1, 45 of 61 OS cases (73.77%) had *GPC3* expression. Based on the immunolabeling intensity, 16 of 61 cases (26.23%) were negative (-), 29 (47.54%) were weakly positive (+), eight (13.11%) were moderately positive (++), and eight (13.11%) were strongly positive (+++) in terms of *GPC3* expression. The percentages of *GPC3*-positive cells in OS tissues were highly variable: XX OS cells were all negative (-), 10%–30% were +, 31%–70% were ++, and >71% were +++. Among the 61 OS cases examined (Figure 2C), 16 (26.23%) were -, eight (13.11%) were +, 22 (36.07%) were ++, and 15 (24.59%) were +++, indicating differential intertumoral and intratumoral *GPC3* expression patterns among OSs. None of the eight OSs surrounding non-cancerous bone specimens showed *GPC3* expression (Figure 3A; Table 1). Statistical analyses revealed that the frequencies of *GPC3* detection were not related to the patient sex, age, or pathological diagnosis (Figure S1).

## 3.3 | Concurrent GPC3 and CD133 expression in OS cells

CD133-positive osteosarcoma cells can exhibit tumor stem-like gene expression patterns and play pivotal roles in tumor progression and chemoresistance.<sup>27,28</sup> IHC staining demonstrated that the CD133 positivity rate was 86.88% among the 61 OS cases but not among the bone samples (0/8). All of the *GPC3*-positive OS cases showed CD133 expression and shared similar intratumoral distribution patterns (Figure 3A,C,  $P_1 = 4.53 \times 10^{-5}$  for intensity and  $P_p = 9.89 \times 10^{-10}$  for percentage), including male patients ( $P_1 = 0.005$ ,  $P_p = 2.2 \times 10^{-5}$ ), female patients ( $P_1 = 4.79 \times 10^{-4}$ ,  $P_p = 6.29 \times 10^{-6}$ ), and those in the younger age group (age < 25 years,  $P_1 = 0.003$ ,  $P_p = 3.75 \times 10^{-7}$ ). Double CD133 and *GPC3* immunofluorescent labeling demonstrated co-expression of *GPC3* and CD133 in the same tumor regions (Figure 3B).

## 3.4 | Successful generation of OS-derived organoids

In this study, 24 OS cases were recruited for organoid modeling. Osteosarcoma organoids were formed within 2 weeks and maintained active growth over months (Figure 4A). The phenotype of the OSOs was usually irregular in shape (Figure 4B). Here, 20 biopsies and 12 surgical tissues were subjected to 3D culture, with organoid formation rates of 95% (19/20) and 91.7% (11/12), respectively. OSOs can be sustained for over 3 months and passaged when

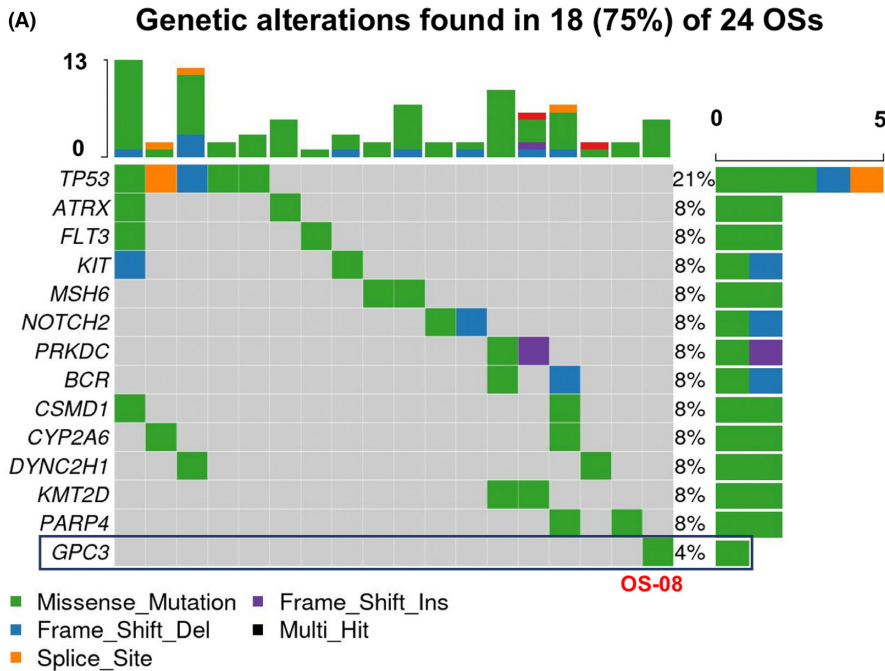
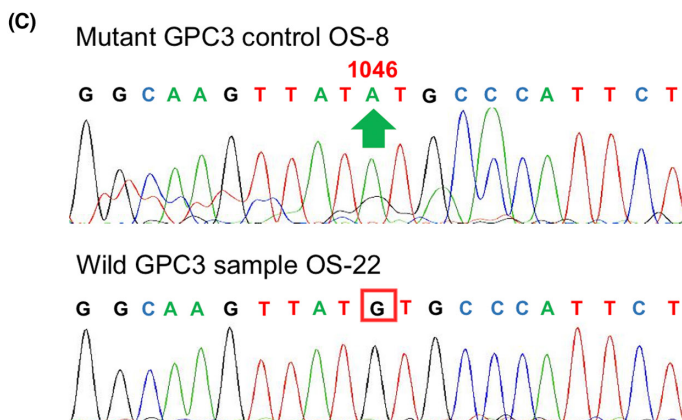
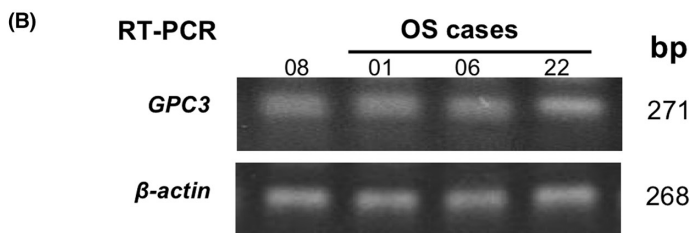


**FIGURE 1** Genomic alterations and GPC expression in osteosarcoma. (A) Osteosarcoma-related gene alterations were detected in 24 osteosarcomas using cancer-targeted next-generation sequencing. Only one patient (OS-8) was found to have a GPC3 mutation. (B) RT-PCR demonstration of GPC3 transcription in OSs.  $\beta$ -Actin was used as a quantitative control, and OS-8 was used as a GPC3-positive control. (C) Sanger sequencing was performed on the GPC3 RT-PCR product of mutant GPC3 (OS-8) and OS-22 as the representative GPC3 wild-type



necessary without apparent phenotypic changes. The expression patterns of the OS biomarkers SOX9 and vimentin, stem cell marker CD133, and GPC3 of the original tumors were well maintained in the corresponding organoids (Figure 4C,D).

### 3.5 | GPC3-dependent response of OSOs to GPC3-Ab treatment

Among the 24 OS cases studied, seven (29.2%) experienced tumor progression after standard high-dose and multidrug combination

therapy, and no reliable alternative treatment was available. Due to the differential expression of GPC3 in patients with OS, organoids derived from one GPC3-negative, one GPC3+, and four GPC3+++ patients were selected for GPC3-targeted therapy (Figure 5A). After 96 h of GPC3-Ab treatment, GPC3+++ organoids showed extensive cell death, the formation of typical apoptotic bodies, and distinct growth arrest (Figure 5B); conversely, GPC3-negative organoids maintained growth under the same experimental conditions, and cell death and TUNEL-labeled nuclei were rarely observed. As shown in Figure 5C, all four GPC3+++ organoids were sensitive to GPC3-Ab with cell inhibition rates of 77.51, 74.40, 76.43, and 92.86% for

**TABLE 1** Immunohistochemical profiling of GPC3 and CD133 expression patterns in individual OS cases according the immunolabeling intensities and the percentage of positive-GPC3 cells

No.	Age	Sex	Location	Intensity		Percentage	
				GPC3	CD133	GPC3	CD133
<b>Fresh specimens</b>							
<b>Osteoblastic OS</b>							
1	8	M	Right femur inferior segment	+++	+++	+++	+++
2	10	M	Left femur	+	+	+++	++
3	15	M	Right knee	-	-	-	-
4	17	M	Left femur	++	+	+	+
5	17	M	Left tibia	+	+++	++	+++
6	18	M	Left tibia superior segment	+++	+++	+++	+++
7	20	M	Right femur	+	+++	++	++
8	20	M	Left humerus	+++	+++	+++	+++
9	21	M	Right humerus	+	+	++	+
10	36	M	Left knee	++	+	+	+
11	37	M	Right femur	-	-	-	-
12	57	M	Left femur	+	++	+++	+++
13	5	F	Left femur	+	+++	+	++
14	8	F	Left femur	+	++	+++	++
15	11	F	Left knee	+	++	++	++
16	14	F	Left femur	+	+	++	+++
17	16	F	Right femur	+	+	+++	+++
18	18	F	Left tibia superior segment	-	-	-	-
19	21	F	Left subscapular lymph node	++	++	+	++
20	23	F	Right femur inferior segment	-	-	-	-
21	63	F	Left femur	-	+	-	++
<b>Chondroblastic OS</b>							
22	23	M	Left pelvic	-	++	-	++
23	39	M	Right femur	+++	+++	+++	+++
24	28	F	Right femur	+	++	+	+
<b>OS microarray</b>							
<b>Osteoblastic OS</b>							
25	12	M	Left femur inferior segment	-	-	-	-
26	14	M	Left face	++	+++	++	+++
27	14	M	Right femur inferior segment	-	++	-	+++
28	15	M	Right femur	+	++	++	+++
29	15	M	Right femur inferior segment	+++	+++	+++	+++
30	15	M	Lower jaw	-	+++	-	++
31	16	M	Right femur	-	+	-	+
32	17	M	Left femur inferior segment	+++	+	++	+++
33	17	M	Right femur superior segment	+	++	+++	+++
34	17	M	Left tibia	+	++	++	+++
35	18	M	Right humerus	++	+	+	+
36	19	M	Left thigh	+	+	++	+++
37	19	M	Right femur (sparse)	-	++	-	++
38	19	M	Left calf fibula	-	+	-	+

(Continues)

TABLE 1 (Continued)

No.	Age	Sex	Location	Intensity		Percentage	
				GPC3	CD133	GPC3	CD133
39	21	M	Popliteal fossa	+	++	++	+++
40	28	M	Left femur	-	++	-	+++
41	33	M	Left upper jaw	+	+	++	+
42	42	M	Left femur	-	-	-	-
43	46	M	Right femur (sparse)	+	++	++	+++
44	51	M	Right fibula	+	++	++	++
45	55	M	Right lower rib	+++	+++	+++	+++
46	12	F	Femur	+	-	+	-
47	12	F	Right femur	+	+++	+++	+++
48	13	F	Left femur inferior segment	+	+	++	++
49	14	F	Left tibia superior segment	-	-	-	-
50	14	F	Left tibia superior segment	-	+	-	+
51	16	F	Left femur	+	+	++	+++
52	18	F	Left distal femur	+++	++	++	++
53	20	F	Right tibia superior segment	+	++	+	++
54	23	F	Left femur	+	++	++	+++
55	28	F	Right femur	++	+++	+++	+++
56	31	F	Left femur	+	+	++	++
57	32	F	Left femur inferior segment	+	+	+++	+++
58	37	F	Right femur inferior segment	+	+	++	+++
59	41	F	Right humerus	++	+++	++	+++
60	56	F	Left frontal	++	+++	++	+++
Fibroblastic OS							
61	27	M	Humerus	+	+++	+++	+++
Tumor-surrounding bone tissues							
62	15	M	Right knee	-	-	-	-
63	28	M	Left femur	-	-	-	-
64	46	M	Right femur	-	-	-	-
65	51	M	Right fibula	-	-	-	-
66	5	F	Left femur	-	-	-	-
67	23	F	Right femur inferior segment	-	-	-	-
68	28	F	Right femur	-	-	-	-
69	63	F	Left femur	-	-	-	-

The deeper of the color represent higher expression of GPC3/ CD133.

OS-21, OS-01, OS-08, and OS-06, respectively. The organoids derived from the four GPC3+++ cases were effectively suppressed by GPC3-Ab (74.40%–92.86%) compared with GPC3+ (23.46%) and GPC3- (10.78%) organoids.

### 3.6 | GPC3-Ab suppressed xenograft growth

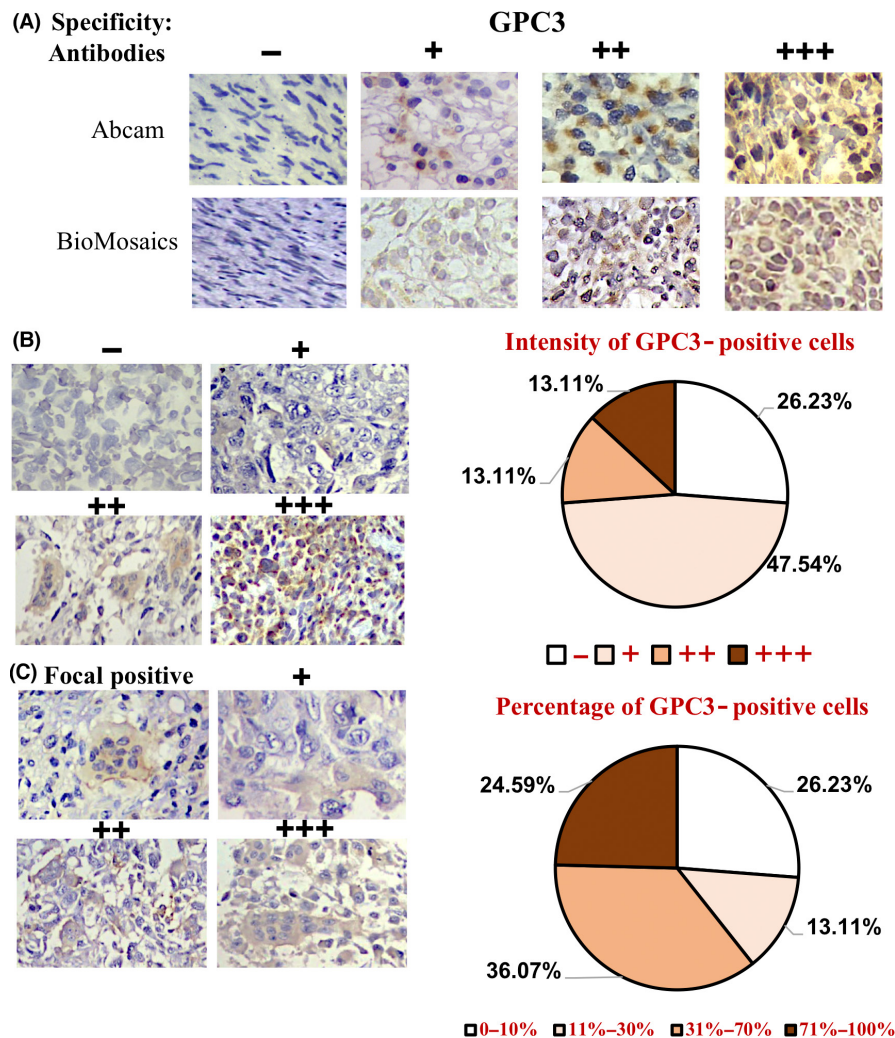
The efficacy of GPC3-Ab in a high GPC3 expressing OSDX-1 model was elucidated. The xenografts demonstrated an 85.1% reduction in tumor volume after treatment with 100 µg GPC3-Ab/mouse three times at 7-day intervals (Figure 6A). In contrast, xenografts

in the control group maintained an average growth rate of 742.0% for the same experimental duration ( $p < 0.0005$ ; Figure 6B). Immunohistochemical staining showed a reduction in GPC3 expression in GPC3-Ab-treated tumors (Figure 6C), accompanied by extensive apoptotic cell death, as shown by TUNEL (Figure 6D).

### 3.7 | Reduction of active $\beta$ -catenin in GPC3-Ab treated OSDX

Immunohistochemical staining and immunofluorescence labeling performed on OSDXs with and without GPC3-Ab treatment

**FIGURE 2** Immunohistochemical profiling of intertumoral and intratumoral GPC3 expression patterns of OS specimens. (A) The specificity results of GPC3 immunohistochemical staining ( $\times 20$ ) ascertained using two anti-GPC3 antibodies from Abcam and BioMosaics. (B) The grades of GPC3 immunohistochemical labeling ( $\times 20$ ) were scored as -, negative; +, weakly positive; ++, moderately positive; and +++, strongly positive, according to the staining intensities (left). (C) Classification of intertumoral GPC3 immunohistochemical labeling ( $\times 20$ ) according to the percentage of GPC3-positive tumor cells: -, all negative; +, focal positive; ++, partially positive; and +++, generally positive (left). IHC data were collected from 61 OS specimens



revealed that the active  $\beta$ -catenin level was distinctly decreased by GPC3-Ab; there was a marked attenuation of  $\beta$ -catenin membranous labeling (Figure 7A). Western blotting further demonstrated that the level of active  $\beta$ -catenin was reduced in GPC3-Ab-treated xenografts in comparison with tumors treated with the antibody diluent (Figure 7B;  $p < 0.005$ ).

## 4 | DISCUSSION

As the most common primary bone malignancy, often linked with poor prognosis, OS frequently occurs in children and adolescents<sup>29</sup> and therefore seriously affects the physical and mental health of this young population.<sup>30</sup> Although a combination of neoadjuvant chemotherapy and surgery can improve the therapeutic outcome of patients with OS and increase the overall survival rate to 65%–70%,<sup>31,32</sup> patients usually suffer from a series of adverse reactions and a decline in the quality of life.<sup>33</sup> Moreover, OS exhibit primary and secondary drug resistance due to intratumoral heterogeneity<sup>34</sup> and/or acquired genetic alterations.<sup>27</sup> As no therapeutic target has so far been identified for OS, this increasingly popular therapy has not yet been applied to OS.<sup>11</sup> Consequently, no alternative option is

available beyond conventional chemotherapy for the treatment of metastatic OS, and amputation must be performed to avoid tumor expansion and spread. There is an urgent need to explore genetic alterations and biomarkers for better management of OS.

GPC3 is an oncofetal protein that plays an active role in the formation and progression of HCCs,<sup>13</sup> hepatoblastomas,<sup>35</sup> lung cancers,<sup>36</sup> and tumors with a background of germline mutations.<sup>37</sup> As GPC3 expression is found in 72% of HCCs and 97% of hepatoblastomas, it has been used as a potential immunotherapeutic target for liver cancers.<sup>13,38</sup> Our NGS analysis performed on the primary and metastatic tumors of an OS case (OS-08) identified a GPC3 point mutation in the primary tumor and its mutation abundance increased 1.68 times in the metastatic tumor with upregulated mutant GPC3 expression.<sup>12</sup> Subsequently, anti-GPC3 was administered to the primary and metastatic OS organoids. This achieved promising inhibitory effects, especially on metastasis,<sup>12</sup> indicating, for the first time, the potential value of GPC3 as a diagnostic biomarker and therapeutic target for OS. These findings encouraged us to profile the frequency of GPC3 mutations and their expression in a large panel of OSs to test this hypothesis.

Loss-of-function mutations in GPC3 have been identified as the genetic defects associated with Simpson-Golabi-Behmel syndrome



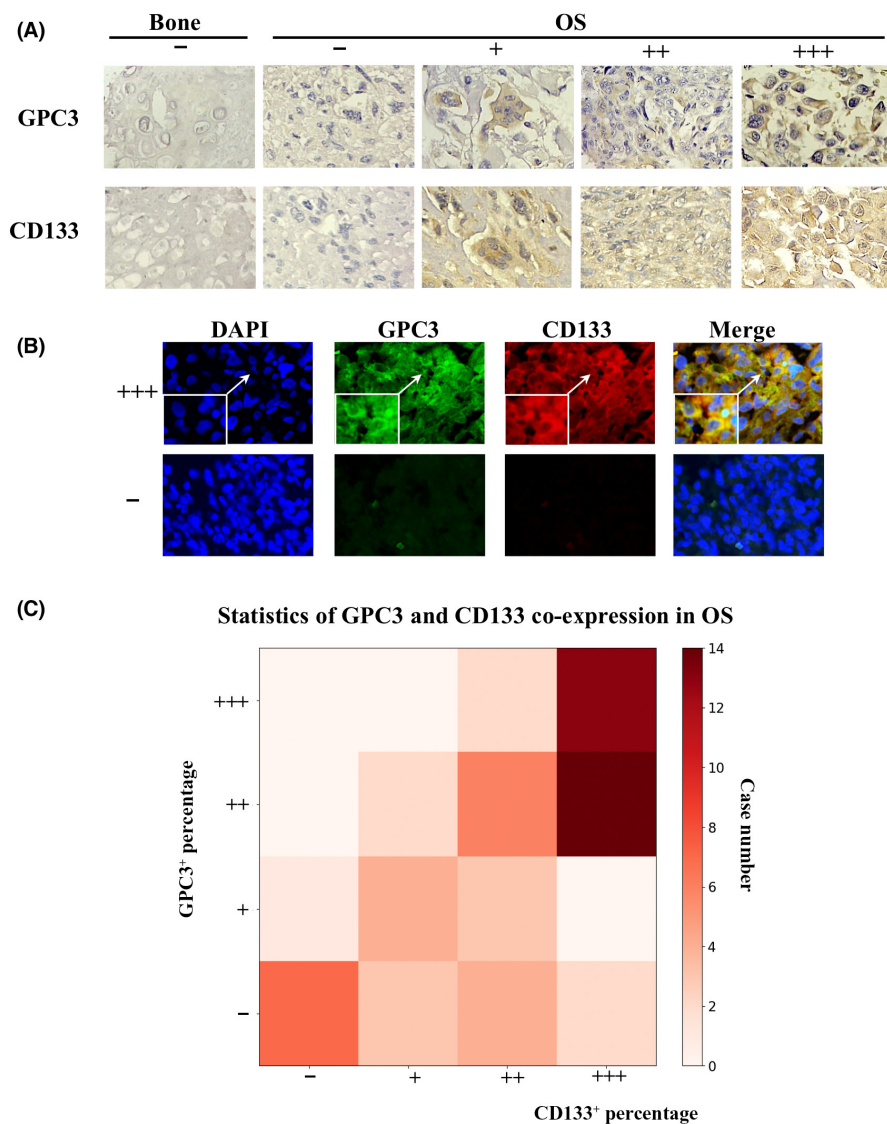


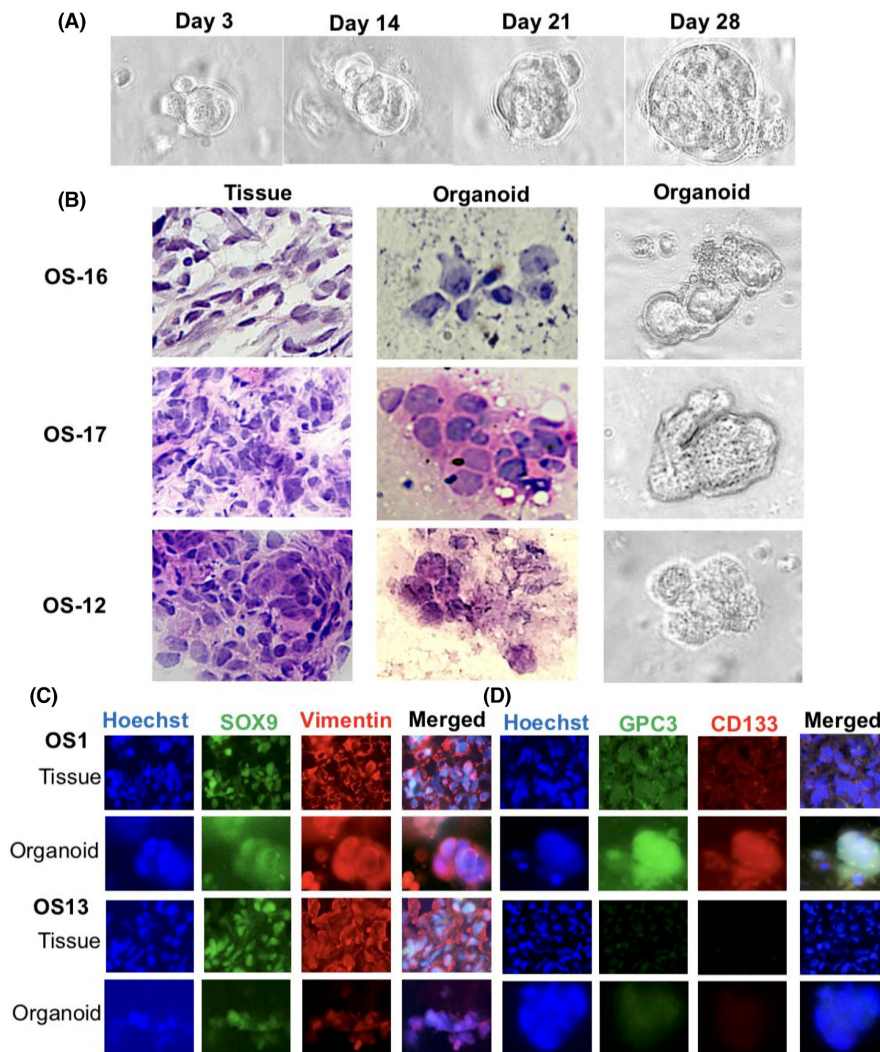
**FIGURE 3** Correlation analyses of GPC3 and CD133 expression in OS tissues and organoids. (A) Immunohistochemical demonstration of frequent GPC3 and CD133 co-expression in OS tissues ( $\times 20$ ). (B) GPC3 and CD133 double immunofluorescent staining ( $\times 20$ ) of GPC3: +++, generally positive; and -, negative OS tissues. Insets represent images with higher magnification ( $\times 40$ ). (C) Percentages of GPC3- and CD133-positive OS cases and their statistical relevance (data from SPSS statistical analysis)

(SGBS) characterized by overgrowth, dysplasia, and multiple congenital anomalies.<sup>39</sup> However, none of the 24 OS patients in this study had SGBS. Unlike other cancer-associated genes, the data concerning GPC3 mutation in human malignancies remain limited. The relevance of GPC3 to HCCs has been evidenced, whereas only GPC3 rs2267531, a promotor single nucleotide polymorphism (SNP) on the X chromosome, rather than a mutation at the functional sites has been found in Egyptian hepatocellular carcinomas.<sup>40</sup> As the first step to investigate the frequency and patterns of GPC3 alterations in OSs, cancer-targeted NGS was performed on 24 OS cases, citing the GPC3 mutated OS-08 as a positive control. These results revealed that GPC3 mutation was undetectable in all OSs, except for OS-08. As the newly checked OS samples were collected from patients of different ages and sexes, we propose that the GPC3 mutation is a rare event rather than a common genetic alteration among OS. GPC3 expression without mutation is commonly found in multiple cancers, for instance, GPC3 is expressed in 72% of HCCs but neither in normal livers nor in noncancerous liver disease.<sup>41</sup> In contrast with the rarity of GPC3 mutations in OSs, GPC3

expression was immunohistochemically observed in 45 out of 61 OS cases (73.77%), a similar frequency to that of HCCs (63%–91%).<sup>13,41</sup> Sanger sequencing was performed on the GPC3 RT-PCR products of GPC3-positive OS samples, which further confirmed that only wild-type GPC3 was transcribed. These findings therefore rule out the involvement of GPC3 mutation in OS formation and progression and provide strong evidence for the potential value of GPC3 in OS management, because GPC3 targeted anti-HCC immunotherapy has so far only been conducted based on the presence of GPC3 expression, not mutation.<sup>15</sup> Epigenetic activation of GPC3 transcription by lncRNA glypican 3 antisense transcript 1 (GPC3-AS1) has been found in HCCs.<sup>42</sup> It would be worthwhile to check the status of GPC3-AS1 in our OS experimental systems and analyze its relevance with GPC3 expression.

Intratumoral heterogeneity is a typical histopathological feature and it is the main therapeutic challenge for OS.<sup>34</sup> In contrast, the outcome of cancer immunotherapy is related to the level and intratumoral distribution pattern of the targeted protein.<sup>43</sup> To evaluate the applicability of GPC3-targeted OS therapy, it is critical to clarify

**FIGURE 4** Establishment and characterization of OS organoids. (A) Bright-field demonstration of continuous growth of an OS-1 organoid ( $\times 40$ ). (B) H&E morphological staining was performed on OS tissues from three cases and the corresponding organoids and bright-field images of the organoids of the matched patients with OS. Tissue,  $\times 20$ ; organoid,  $\times 40$ . (C) Double immunofluorescent labeling of OS-specific biomarkers, SOX9 and vimentin, on OS tissues and organoids with (OS-1) and without (OS-13) GPC3 expression. Tissue,  $\times 20$ ; organoid,  $\times 40$ . (D) GPC3 and CD133 double immunofluorescent labeling of paired OS tissue and organoids of OS-1 and OS-13. Tissue,  $\times 20$ ; organoid,  $\times 40$



the intensity of GPC3 production, particularly the distribution patterns of GPC3-expressing cells in OS tissues. Immunohistochemical staining of fresh OS tissue and tumor microarray revealed that GPC3 levels were different among the 61 OS cases: negative (15/61 cases), weakly positive (29/61 cases), moderately positive (9/61 cases), and strongly positive (8/61 cases), suggesting differential intertumoral GPC3 expression and demonstrating the necessity for individualized GPC3-targeted therapy. More importantly, the intratumoral distribution of GPC3-positive tumor cells was variable among the 45 GPC3-positive cases in the patterns of focal positive (10%–30%) in eight cases (17.78%) to generally positive (>70%) in 15 cases (33.33%), demonstrating the cellular heterogeneity of OSs, even in terms of GPC3 expression. These results also indicated that the efficacy of anti-GPC3 therapy against OS may be case- or GPC3-dependent. CD133 is known to be a biomarker of OS.<sup>44</sup> It plays active roles in OS initiation and progression<sup>27</sup> and confers drug resistance to OS cells.<sup>45</sup> Parallel immunohistochemical staining and double immunofluorescent labeling demonstrated concurrent CD133 expression (97.8%; 44/45) in GPC3-positive OS, while CD133<sup>-</sup>/GPC3<sup>+</sup> cells accounted for only 2.2%. These findings indicate that GPC3-targeted therapy may also attack CD133-positive stem-like OS cells and

therefore achieve double-gain therapeutic efficacy. It would be of practical significance to address these issues using GPC3-positive and GPC3-negative OS-derived organoids as preclinical therapeutic models.

Patient-derived tumor organoids (PDOs) formed under suitable three-dimensional culture conditions can maintain the basic molecular and biological features of their original tumors.<sup>46</sup> Therefore, the results obtained from PDOs would have translational value, especially in personalized cancer treatment.<sup>47</sup> In this study, a panel of PDOs was successfully generated from 24 OS cases with different GPC3 expression patterns, therefore providing an ideal *ex vivo* platform for GPC3-oriented therapy. To elucidate the applicability of the GPC3-targeted strategy for OS, PDOs derived from one GPC3-negative and four GPC3-positive cases were treated with anti-GPC3 antibody. The GPC3-positive organoids were sensitive to the anti-GPC3 antibody as they showed infrequent EdU-labeled cells and increased apoptotic fractions in comparison with their antibody diluent-treated counterparts. In contrast, the GPC3-negative OSOs remained intact under the same experimental conditions. These results confirmed that GPC3-targeted therapy is selectively effective for GPC3-expressing OS cases, irrespective of the type (wild or

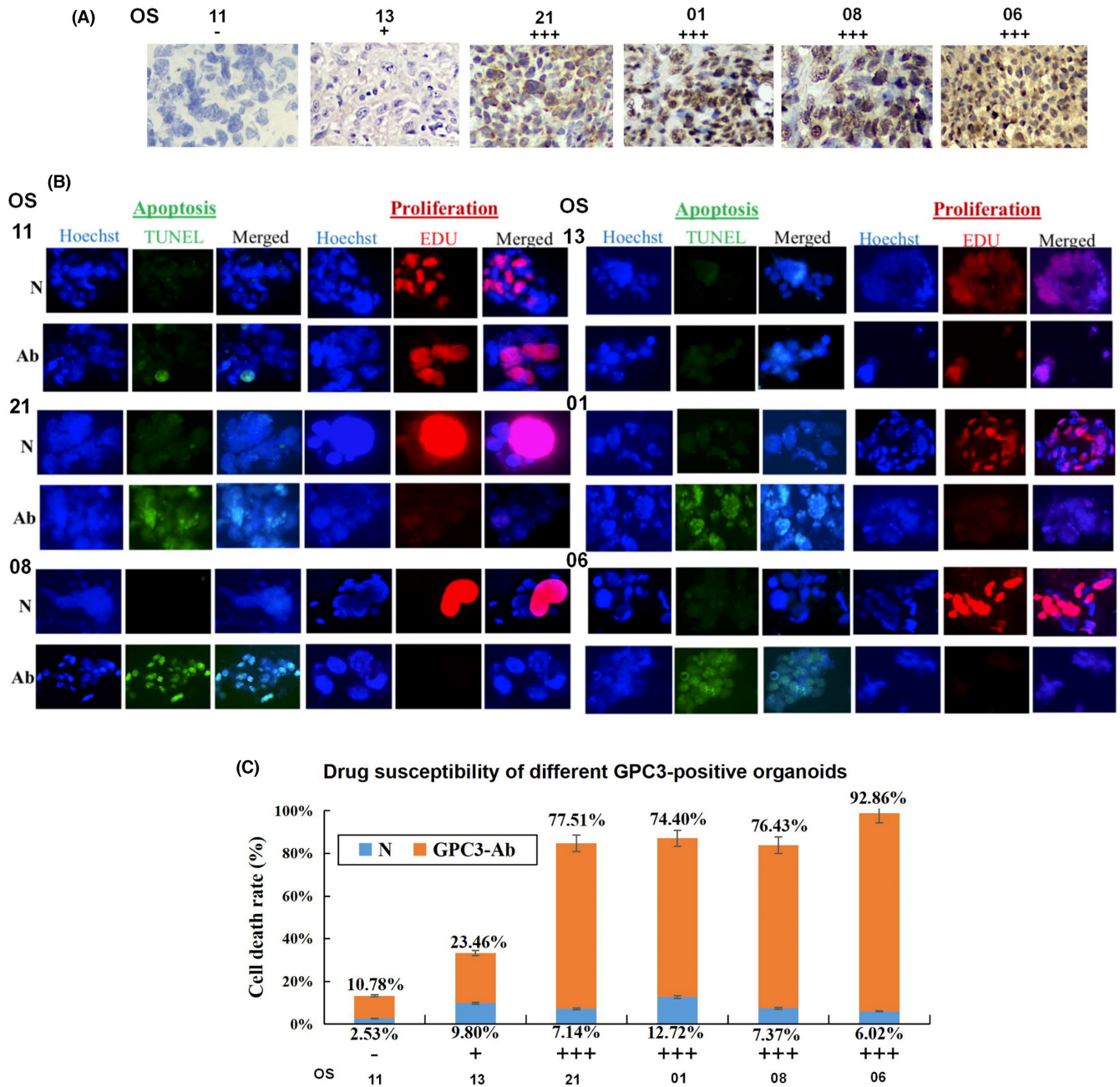


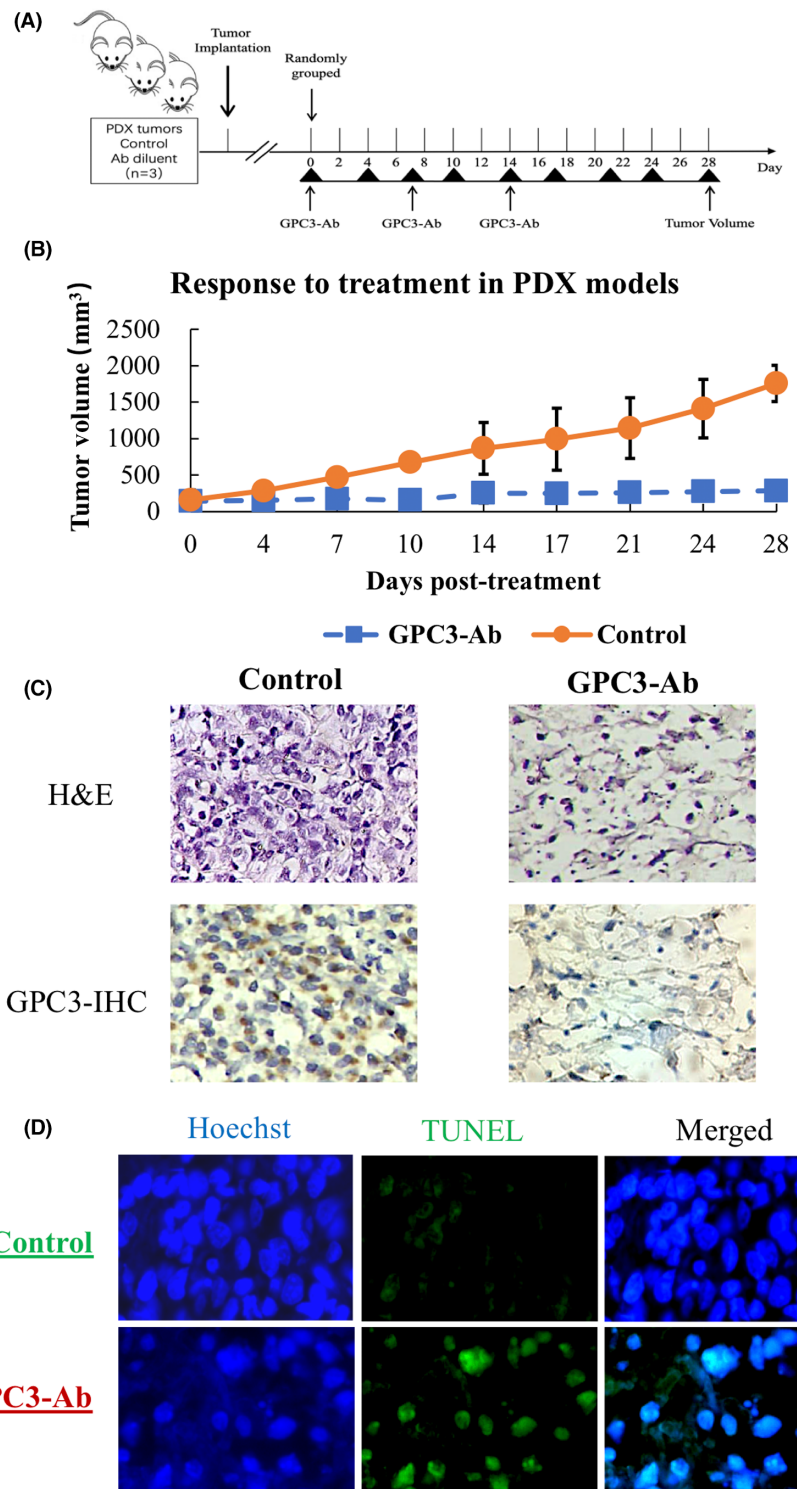
**FIGURE 5** GPC3 targeted therapy performed on OS organoids with different GPC3 expression patterns. (A) Immunohistochemical ( $\times 20$ ) demonstration of differential GPC3 expression in OS tissues used for organoid culture. (B) Evaluation of apoptosis (TUNEL) and proliferation (EdU) of GPC3-antibody (GPC3-Ab)-treated OS organoids with different levels of GPC3 expression ( $\times 40$ ). (C) The response of OS organoids to GPC3-Ab treatment in a GPC3-related manner

mutant) of GPC3 proteins they produce. This notion is further supported by our *in vivo* findings that the growth of GPC3-expressing OSDXs is efficiently inhibited at an average rate of 85.1% and extensive apoptotic cell death in tumor tissues after three administrations of anti-GPC3 antibody at 1-week intervals. These *ex vivo* and *in vivo* data suggest the feasibility of a GPC3-targeted strategy for personalized OS therapy. The anti-tumor effects of IL15 and/or IL21 enhanced glypican-3-CAR T cells (21.15.GPC3-CAR T cells) have been demonstrated in HCC cell lines, as well as in murine xenograft models of GPC3<sup>+</sup> tumors.<sup>48</sup> We are currently using this type

of GPC3-CAR T cell to treat the OSDX model as the next round of preclinical trials for the practical application of personalized osteosarcoma treatment.

The biological effects of GPC3 are mediated via the canonical Wnt/ $\beta$ -catenin signaling pathway.<sup>49</sup> GPC3 attracts and concentrates Wnt ligands to the cancer cell surface and subsequently activates the Wnt/ $\beta$ -catenin pathway,<sup>25</sup> as evidenced in human HCCs.<sup>49</sup> According to the literature, the Wnt/ $\beta$ -catenin pathway plays a key role in osteosarcoma development and progression.<sup>50,51</sup> A high level of  $\beta$ -catenin expression in OS tissues is closely related to lung

**FIGURE 6** GPC3 targeted therapy performed on a high GPC3 expression OSDX. (A) Schematic of in vivo GPC3-Ab treatment used on the OSDX platform. (B) Tumor volume over time in a high GPC3 expression OSDX mouse model administered three times weekly with the control (antibody diluent) or GPC3-Ab (100 $\mu$ g/mouse). Data points represent mean ( $n = 5$ )  $\pm$  standard error. (C) Images ( $\times 20$ ) of H&E- and GPC3-oriented immunohistochemical staining of OSDX tissues with and without (control) GPC3-Ab treatment (GPC3-Ab). (D) TUNEL apoptotic cell labeling ( $\times 20$ ) of OSDX tissues without (control) or with GPC3-Ab treatment (GPC3-Ab)



metastasis and therefore results in a poor prognosis.<sup>52</sup> In this study, we demonstrated that GPC3 proteins are co-localized with active  $\beta$ -catenin on OS cell membranes. It is reasonable to propose that GPC3 proteins may bind to Wnt molecules to form Wnt/frizzled/ $\beta$ -catenin complexes, which inhibit  $\beta$ -catenin degradation via axin dysfunction, leading to activation of the canonical Wnt/ $\beta$ -catenin pathway and finally OS progression. This hypothesis is supported by our findings that anti-GPC3 antibody efficiently prevents  $\beta$ -catenin membranous localization by inhibiting  $\beta$ -catenin activation, leading to in vivo and

in vitro growth arrest and apoptosis of GPC3-positive rather than GPC3-negative PDOs.

Overall, frequent GPC3 expression (73.77%) rather than mutation (4%) was observed in 61 OS cases. Co-expression of GPC3 and CD133 was detected in 97.8% (44/45) of the GPC3-positive OS tissues and their PDOs, making GPC3-targeted anti-OS therapy more meaningful. The suppressive effects of anti-GPC3 antibody on GPC3-expressing (rather than GPC3-negative) OS PDOs suggest that this therapeutic strategy is a promising approach to improve OS

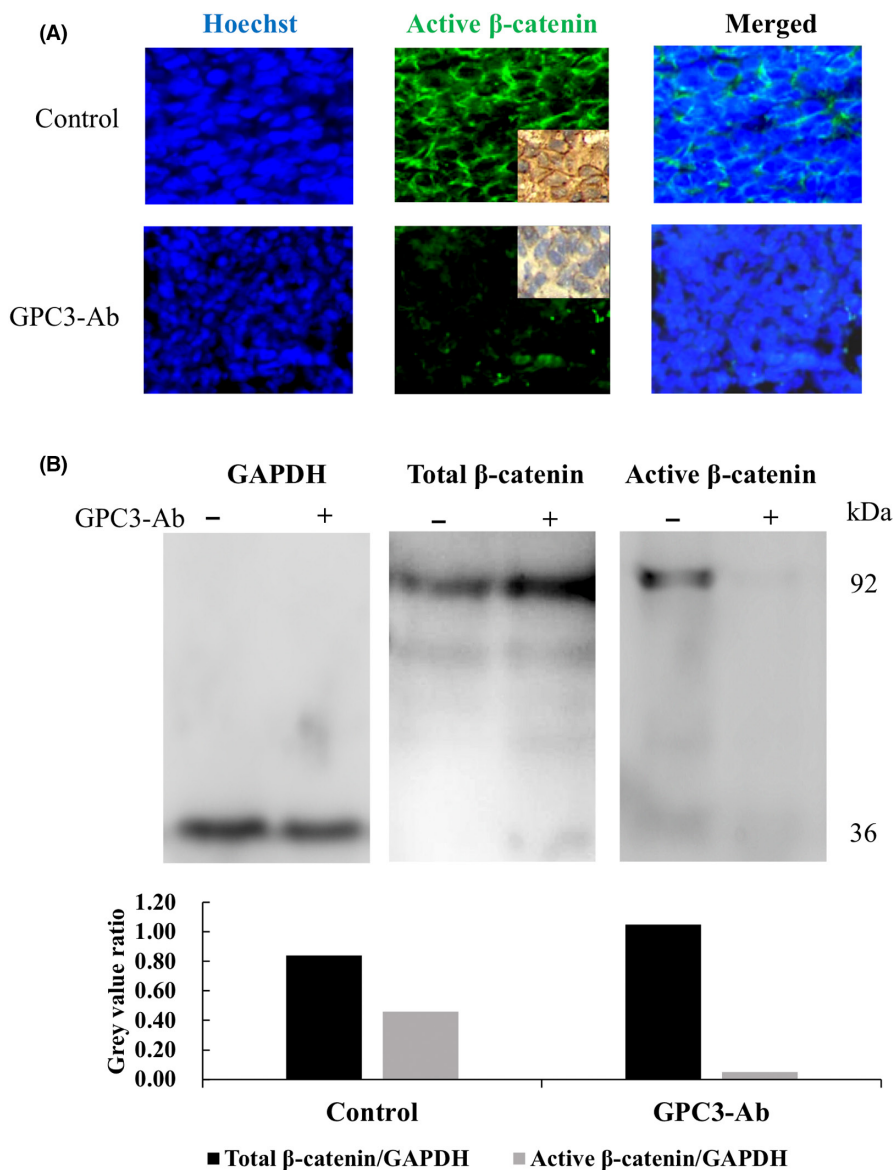


**FIGURE 7** Reduced active  $\beta$ -catenin production and membranous localization in GPC3-Ab-treated OSDX tissues. (A) Immunofluorescence and immunohistochemical (insets) illustration of active  $\beta$ -catenin in OSDX tissues with and without (control) GPC3-Ab treatment ( $\times 20$ ). (B) Western blot analysis of the total and active  $\beta$ -catenin levels in OSDX tissues with and without GPC3-Ab treatment. GAPDH was used as a quantitative control for analysis (gray)

prognosis in a GPC3-related personalized manner. Growth suppression via anti-GPC3 antibody-treated GPC3-expressing OSDX suggests the feasibility of GPC3-targeted therapy. It is important to trial the response of OSDXs with different GPC3 expression patterns to anti-GPC3 antibody and/or GPC3-CAR T immunotherapy and clinical trials are the next step to further strengthen this hypothesis.

#### ACKNOWLEDGMENTS

The authors wish to acknowledge the doctors of the Department of Clinical Pathology, Guangdong Provincial People's Hospital for their assistance in providing the osteosarcoma paraffin specimens as well as the experimental support provided by Ms. Xuan Luo in the Jingke BioMed Laboratory.

#### DISCLOSURE

The authors are not Editors or Editorial Board Members of Cancer Science. The corresponding authors Yu Zhang\* and Jia Liu\* declare that the authors have no conflicts of interest.

#### FUNDING

This work was supported by grants from the National Natural Science Foundation of China (No. 31771038) and the High-level Hospital Construction Project of China (No. DFJH201905) to Dr. Yu Zhang. In addition, it was supported by grants from the National Natural Science Foundation of China (No. 81272786 and 81450016) and the Special Fund of South China University of Technology from the Central Government of China to Dr. Jia Liu.

#### ETHICAL APPROVAL

Approval of the research protocol: This study protocol was reviewed and approved by the Research Ethics Committee of Guangdong Provincial People's Hospital, Guangdong Academy of Medical Sciences.

Registration No.: the registration number is No. GDREC2020093A.

Informed Consent: the samples used in this study were collected from the Department of Orthopedic Oncology, Guangdong People's Hospital, Guangzhou, China, and written informed consent was

obtained from the patients and/or their immediate relatives using recognized guidelines.

**Animal Study:** the animal study was conducted in accordance with the ARRIVE guidelines, the National Research Council's Guide for the Care and Use of Laboratory Animals, and approval of Laboratory Animal Research Center of South China University of Technology (AEC No. 2019024).

## ORCID

Jia Liu  <https://orcid.org/0000-0002-4920-6013>

## REFERENCES

- Rojas GA, Hubbard AK, Diessner BJ, Ribeiro KB, Spector LG. International trends in incidence of osteosarcoma (1988-2012). *Int J Cancer*. 2021;149:1044-1053.
- Isakoff MS, Bielack SS, Meltzer P, Gorlick R. Osteosarcoma: current treatment and a collaborative pathway to success. *J Clin Oncol*. 2015;33:3029-3035.
- Siegel RL, Miller KD, Jemal A. Cancer statistics, 2020. *CA Cancer J Clin*. 2020;70:7-30.
- Messerschmitt PJ, Garcia RM, Abdul-Karim FW, Greenfield EM, Getty PJ. Osteosarcoma. *J Am Acad Orthop Surg*. 2009;17:515-527.
- Whelan JS, Davis LE. Osteosarcoma, chondrosarcoma, and chordoma. *J Clin Oncol*. 2018;36:188-193.
- Jaffe N, Puri A, Gelderblom H. Osteosarcoma: evolution of treatment paradigms. *Sarcoma*. 2013;2013:203531.
- Siravegna G, Mussolin B, Buscarino M, et al. Clonal evolution and resistance to EGFR blockade in the blood of colorectal cancer patients. *Nat Med*. 2015;21:827.
- Swanton C, Soria JC, Bardelli A, et al. Consensus on precision medicine for metastatic cancers: a report from the MAP conference. *Ann Oncol*. 2016;27:1443-1448.
- Mariotto AB, Etzioni R, Hurlbert M, Penberthy L, Mayer M. Estimation of the number of women living with metastatic breast cancer in the United States. *Cancer Epidemiol Biomarkers Prev*. 2017;26:809-815.
- El-Deiry WS, Goldberg RM, Lenz HJ, et al. The current state of molecular testing in the treatment of patients with solid tumors, 2019. *CA Cancer J Clin*. 2019;69:305-343.
- Kansara M, Teng MW, Smyth MJ, Thomas DM. Translational biology of osteosarcoma. *Nat Rev Cancer*. 2014;14:722-735.
- Nie JH, Yang T, Li H, et al. Identification of GPC3 mutation and up-regulation in a multidrug resistant osteosarcoma and its spheroids as therapeutic target. *J Bone Oncol*. 2021;30:100391.
- Zhou F, Shang W, Yu X, Tian J. Glypican-3: a promising biomarker for hepatocellular carcinoma diagnosis and treatment. *Med Res Rev*. 2018;38:741-767.
- Shimizu Y, Suzuki T, Yoshikawa T, Endo I, Nakatsura T. Next-generation cancer immunotherapy targeting glypican-3. *Front Oncol*. 2019;9:248.
- Yu M, Luo H, Fan M, et al. Development of GPC3-specific chimeric antigen receptor-engineered natural killer cells for the treatment of hepatocellular carcinoma. *Mol Ther*. 2018;26:366-378.
- Lukonin I, Serra D, Challet Meylan L, et al. Phenotypic landscape of intestinal organoid regeneration. *Nature*. 2020;586:275-280.
- He A, Huang Y, Cheng W, et al. Organoid culture system for patient-derived lung metastatic osteosarcoma. *Med Oncol*. 2020;37:105.
- Li H, Sun Y, Kong QY, et al. Combination of nucleic acid and protein isolation with tissue array construction: using defined histologic regions in single frozen tissue blocks for multiple research purposes. *Int J Mol Med*. 2003;12:299-304.
- Yoshida S, Celaire J, Pace C, et al. Delay in diagnosis of primary osteosarcoma of bone in children: have we improved in the last 15 years and what is the impact of delay on diagnosis? *J Bone Oncol*. 2021;28:100359.
- Di Tommaso L, Franchi G, Park YN, et al. Diagnostic value of HSP70, glypican 3, and glutamine synthetase in hepatocellular nodules in cirrhosis. *Hepatology*. 2007;45:725-734.
- Ueda T, Kumagai A, Iriguchi S, et al. Non-clinical efficacy, safety and stable clinical cell processing of induced pluripotent stem cell-derived anti-glypican-3 chimeric antigen receptor-expressing natural killer/innate lymphoid cells. *Cancer Sci*. 2020;111:1478-1490.
- Li H, Zhang YC, Tsuchihashi Y. Invasion and metastasis of SY86B human gastric carcinoma cells in nude mice. *Jpn J Cancer Res*. 1988;79:750-756.
- Capurro MI, Xiang YY, Lobe C, Filmus J. Glypican-3 promotes the growth of hepatocellular carcinoma by stimulating canonical Wnt signaling. *Cancer Res*. 2005;65:6245-6254.
- Takai H, Kato A, Kinoshita Y, et al. Histopathological analyses of the antitumor activity of anti-glypican-3 antibody (GC33) in human liver cancer xenograft models: the contribution of macrophages. *Cancer Biol Ther*. 2009;8:930-938.
- Gao W, Kim H, Feng M, et al. Inactivation of Wnt signaling by a human antibody that recognizes the heparan sulfate chains of glypican-3 for liver cancer therapy. *Hepatology*. 2014;60:576-587.
- Li J, Xu C, Lee HJ, et al. A genomic and epigenomic atlas of prostate cancer in Asian populations. *Nature*. 2020;580:93-99.
- Czarnecka AM, Synoradzki K, Firlej W, et al. Molecular biology of osteosarcoma. *Cancer*. 2020;12:2130.
- Subramaniam D, Angulo P, Ponnurangam S, et al. Suppressing STAT5 signaling affects osteosarcoma growth and stemness. *Cell Death Dis*. 2020;11:149.
- Mirabello L, Troisi RJ, Savage SA. Osteosarcoma incidence and survival rates from 1973 to 2004: data from the surveillance, epidemiology, and end results program. *Cancer*. 2009;115:1531-1543.
- Sachsenmaier SM, Ipach I, Kluba T. Quality of life, physical and mental status and contentment of patients with localized soft tissue or bone sarcoma: a questionnaire analysis. *Orthop Rev*. 2015;7:5920.
- Mirabello L, Troisi RJ, Savage SA. International osteosarcoma incidence patterns in children and adolescents, middle ages and elderly persons. *Int J Cancer*. 2009;125:229-234.
- Kager L, Zoubek A, Potschger U, et al. Primary metastatic osteosarcoma: presentation and outcome of patients treated on neoadjuvant cooperative osteosarcoma study group protocols. *J Clin Oncol*. 2003;21:2011-2018.
- Collins M, Wilhelm M, Conyers R, et al. Benefits and adverse events in younger versus older patients receiving neoadjuvant chemotherapy for osteosarcoma: findings from a meta-analysis. *J Clin Oncol*. 2013;31:2303-2312.
- Lilienthal I, Herold N. Targeting molecular mechanisms underlying treatment efficacy and resistance in osteosarcoma: a review of current and future strategies. *Int J Mol Sci*. 2020;21:6885.
- Zhou S, O'Gorman MR, Yang F, Andresen K, Wang L. Glypican 3 as a serum marker for hepatoblastoma. *Sci Rep*. 2017;7:45932.
- Chen C, Huang X, Ying Z, et al. Can glypican-3 be a disease-specific biomarker? *Clin Transl Med*. 2017;6:18.
- Gallo A, Fankhauser C, Hermanns T, et al. HNF1beta is a sensitive and specific novel marker for yolk sac tumor: a tissue microarray analysis of 601 testicular germ cell tumors. *Mod Pathol*. 2020;33:2354-2360.
- Batra SA, Rathi P, Guo L, et al. Glypican-3-specific CAR T cells co-expressing IL15 and IL21 have superior expansion and antitumor activity against hepatocellular carcinoma. *Cancer Immunol Res*. 2020;8:309-320.

39. Vuillaume ML, Moizard MP, Rossignol S, et al. Mutation update for the GPC3 gene involved in Simpson-Golabi-Behmel syndrome and review of the literature. *Hum Mutat.* 2018;39:790-805.
40. Motawi TMK, Sadik NAH, Sabry D, Shahin NN, Fahim SA. rs2267531, a promoter SNP within glypican-3 gene in the X chromosome, is associated with hepatocellular carcinoma in Egyptians. *Sci Rep.* 2019;9:6868.
41. Capurro M, Wanless IR, Sherman M, et al. Glypican-3: a novel serum and histochemical marker for hepatocellular carcinoma. *Gastroenterology.* 2003;125:89-97.
42. Zhu XT, Yuan JH, Zhu TT, Li YY, Cheng XY. Long noncoding RNA glypican 3 (GPC3) antisense transcript 1 promotes hepatocellular carcinoma progression via epigenetically activating GPC3. *FEBS J.* 2016;283:3739-3754.
43. Shi D, Shi Y, Kaseb AO, et al. Chimeric antigen receptor-glypican-3 T-cell therapy for advanced hepatocellular carcinoma: results of phase I trials. *Clin Cancer Res.* 2020;26:3979-3989.
44. Xu N, Kang Y, Wang W, Zhou J. The prognostic role of CD133 expression in patients with osteosarcoma. *Clin Exp Med.* 2020;20:261-267.
45. Gui K, Zhang X, Chen F, et al. Lipid-polymer nanoparticles with CD133 aptamers for targeted delivery of all-trans retinoic acid to osteosarcoma initiating cells. *Biomed Pharmacother.* 2019;111:751-764.
46. Nikolaev M, Mitrofanova O, Broguiere N, et al. Homeostatic mini-intestines through scaffold-guided organoid morphogenesis. *Nature.* 2020;585:574-578.
47. Driehuis E, Kolders S, Spelier S, et al. Oral mucosal organoids as a potential platform for personalized cancer therapy. *Cancer Discov.* 2019;9:852-871.
48. Nguyen R, Moustaki A, Norrie JL, et al. Interleukin-15 enhances anti-GD2 antibody-mediated cytotoxicity in an orthotopic PDX model of neuroblastoma. *Clin Cancer Res.* 2019;25:7554-7564.
49. Li D, Li N, Zhang YF, et al. Persistent polyfunctional chimeric antigen receptor T cells that target glypican 3 eliminate orthotopic hepatocellular carcinomas in mice. *Gastroenterology.* 2020;158:2250-2265 e2220.
50. Danieau G, Morice S, Redini F, Verrecchia F, Royer BB. New insights about the Wnt/beta-catenin signaling pathway in primary bone tumors and their microenvironment: a promising target to develop therapeutic strategies? *Int J Mol Sci.* 2019;20:3751.
51. Chen J, Liu G, Wu Y, et al. CircMYO10 promotes osteosarcoma progression by regulating miR-370-3p/RUVBL1 axis to enhance the transcriptional activity of beta-catenin/LEF1 complex via effects on chromatin remodeling. *Mol Cancer.* 2019;18:150.
52. Liu W, Zhao Z, Wang Y, et al. Dioscin inhibits stem-cell-like properties and tumor growth of osteosarcoma through Akt/GSK3/beta-catenin signaling pathway. *Cell Death Dis.* 2018;9:343.

#### SUPPORTING INFORMATION

Additional supporting information can be found online in the Supporting Information section at the end of this article.

**How to cite this article:** Nie J-H, Yang T, Li H, et al. Frequently expressed glypican-3 as a promising novel therapeutic target for osteosarcomas. *Cancer Sci.* 2022;113:3618-3632. doi: [10.1111/cas.15521](https://doi.org/10.1111/cas.15521)